

Enhancement of Signaling Processes on Membrane through Molecular Crowding

Masashi Fujii,*Hiraku Nishimori, and Akinori Awazu

Department of Mathematical and Life Sciences, Hiroshima University,
Kagami-yama 1-3-1, Higashi-Hiroshima, Japan

Abstract

We investigated the influences of molecular crowding on biochemical reaction processes on two-dimensional surfaces, using the model of signal-transduction processes on biomembranes. We performed simulations of the two-dimensional cell-based model, which describes the reactions and diffusions of the receptors, signaling proteins, target proteins, and crowders, on the cell membrane. The signaling proteins are activated by receptors and induce target proteins to unbind from the membrane. We found that the reaction rates of two-dimensional systems consistently exhibit a maximum at a high volume fraction of molecules, such that two molecules in the vicinity cannot easily exchange their positions. We further demonstrated that molecular crowding influences the hierarchical molecular distributions throughout the reaction process. The signaling proteins tend to surround the receptors, and the target proteins tend to become distributed around the signaling protein-receptor clusters. This distribution accelerates the receptor–signaling protein and signaling protein–target protein reactions. Thus, molecular crowding frequently enhances reactions on two-dimensional surfaces, but restricts reactions in three-dimensional bulk systems.

Keywords: signal transduction; molecular crowding; cell-based model

*Address reprint requests to Masashi Fujii, Dept. of Mathematical and Life Sciences, Hiroshima University, Kagami-yama 1-3-1, Higashi-Hiroshima, Japan 735-8526. E-mail: mfujii0123@hiroshima-u.ac.jp

INTRODUCTION

Several living systems can sense and respond to environmental variations by means of internal biochemical processes. The adaptations of several cells and the cell fate of multicellular organisms (e.g., cell proliferation, differentiation, and apoptosis) are typical behaviors regulated by intracellular signal-transduction processes (1–6). This simultaneous progression of several internal biochemical processes requires the synthesis and interaction of a number of different proteins on several biomembranes and in the cytoplasm involving several macromolecules, the cytoskeleton, and internal organs.

Recent studies suggest that individual cells contain a much higher volume fraction of macromolecules than do cells in typical *in vitro* conditions (7–26). In fact, the total volume fraction of macromolecules in a typical cell is estimated to be 50–400mg/mL, whereas that under typical *in vitro* conditions is estimated as 1–10mg/mL (7). This situation of such a high volume fraction of molecules, commonly called “molecular crowding”, give rise to extreme spatial restrictions. Thus, the diffusion and deformations (reaction) of molecules in the cytoplasm are highly suppressed (8–21). Such spatial restrictions are also expected to enhance protein folding (22, 23), formation and stabilization of intracellular architecture (24), and processive phosphorylation of erk map kinase (25, 26).

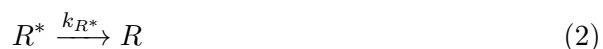
The transduction of signals from the extracellular environment starts with the activation of receptor and signaling proteins on the cell membrane. Thus, the sensing and response of cells is dependent on rapid and appropriate transport and reaction of signaling molecules in a two-dimensional space. Recently, imaging measurements of macromolecules on the cell membrane have been extensively performed (27–37). In some of these measurements, subdiffusive motion was revealed to be the typical motion of membrane proteins (34–37). This observation implies the existence of some type of intrinsic membrane domain like raft or nonimaged molecules, which restrict the observed molecular motions by means of their excluded volumes. Thus, to uncover the functional performance and mechanisms of the upstream part of the signal-transduction processes, the influences of molecular crowding on the reaction and diffusion dynamics of two-dimensional systems should be investigated.

Here, we investigated the influences of molecular crowding on biochemical processes, using an ideal model of typical signal-transduction processes on biomembrane, which mimic the EGF-RAS-RAF and G-protein (guanine nucleotide-binding proteins) signaling process. This model consists of active and inactive receptors (R^* and R), active and inactive signaling proteins (S^* and S), binding and unbinding target proteins (T and T^*), and nonreactive molecules (crowder, C), which diffuse and react in a two-dimensional space. The signal-transduction process is described as the cascade from the activation of receptors to the unbinding of activated target proteins from the membrane, through the following reactions (Fig. 1).

(A) The active/inactive receptor autonomously becomes inactive/active with the reaction rate k_R/k_{R^*} , respectively, described by



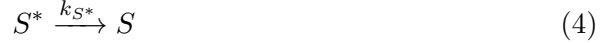
and



(B) When the inactive signaling protein makes contact with an active receptor, this signaling protein is activated with the reaction rate k_S . The active signaling protein autonomously becomes inactive with the reaction rate k_S^* . These processes are described by



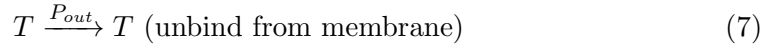
and



(C) The target protein autonomously binds to the membrane with the probability P_{in} . When a target protein makes contact with an active signaling protein, this target protein is activated with the reaction rate k_T . Here, the target protein unbinds from the membrane as soon as it is activated. In the absence of activation, the target protein unbinds from the membrane with the reaction rate P_{out} . These processes are described by



and



Here, each of molecules, R , R^* , S^* , S , T , and C has its own volume. These molecules move randomly under the restriction of their excluded volume, where the distance between the centers of two molecules cannot be smaller than the sum of their Van der Waals radii. For simplicity, we assume that the radius of each molecular is uniform.

A recently recognized feature of molecular crowding is that the reaction activity of the system exhibits a maximum at an appropriate total volume fraction of the system (9, 14, 15, 18). Such an appropriate volume fraction is estimated as not too large as to restrict molecular diffusion, but large enough to cause frequent collisions between reactive molecules. Recently, mean field analysis based on consideration of the balance between the diffusivity and collision rate of molecules has provided an explanation for the volume-fraction-dependent reaction activity of some three-dimensional bulk reaction systems (9).

Here, we propose that the volume-fraction-dependent aspects of reaction processes on two-dimensional surface should deviate considerably from those of bulk reaction systems. Indeed, when analyzed by mean-field approximation, the present reaction system shows almost the same volume-fraction-dependent aspects as do those of the previous studies (14, 26) (see Appendix). Here, the signal flow estimated as the rate of activation of T , exhibits a maximum value at an intermediate total volume fraction of the molecules. On the other hand, the simulation results of the present reaction system in a two-dimensional space indicate that the signal flow exhibits a maximum at a higher volume fraction of molecules, such that two molecules in the vicinity cannot easily exchange their position (see Fig. 4 ; Results and Discussion for details).

The present simulation further show that, in the case exhibiting the maximum signal flow, spontaneous organization of spatially ordered molecular distribution

takes place. Thus, the signal proteins surrounding the receptors are rapidly activated, and the target proteins distributed around the receptor-signaling protein cluster and are rapidly activated. In this way, the formations of spatial structure that cannot be assumed in mean-field approximation provide the dominant contribution to the reaction activity. As mentioned in the following sections, such a spatial structure is formed and sustained by the typical processes of signal transductions on the membrane, e.g., the binding, reactions, and unbinding of molecules, and also by the inferences of molecular crowding.

MODEL AND SIMULATION METHOD

Cell-based model

Here, we have used the two-dimensional cell-based model (38, 39) to describe the diffusion and reactions of the active and inactive receptors (R^* and R), the active and inactive signaling proteins (S^* and S), the binding target proteins (T), and the crowders (C) on the membrane. The space is divided into N two-dimensional hexagonal cells as shown in Fig. 2. Each cell can contain only one molecule, which represents the excluded volume effect among molecules. Each molecule randomly hops from one cell to a neighboring empty cell or reacts in the manner indicated by Eqs. 1, 2, 4, 5 or 7. Here, reactions 1, 2, 4, and 7 occur spontaneously with each reaction rate, whereas two-body reactions 3 and 6 occur when two corresponding molecules exist in adjacent cells. In the empty cell, reaction 5 occurs on its rate P_{in} ; here, the crowder does not react.

As the index of molecular crowding, we define “occupancy” as [Total number of molecules in the system]/ N . The volume fraction, which has frequently been used as the index of molecular crowding in recent arguments, is roughly estimated from the occupancy, under the following assumptions. First we assume that all molecules are almost the same size. Second, the size of each cell is considered sufficiently large compared with those of the molecules, that indicate, the center of each molecule can fluctuate in each cell, and two molecules in neighboring cells do not maintain contact with each other. Third, the size of each cell must be small enough for the distance between two molecules in neighboring cells to be always smaller than the molecular diameter, to avoid the possibility of invasion of a molecule between two neighboring molecules. For example, we assume that the length of the edge of each hexagonal cell is $\sim 1.7 \times$ [molecular diameter], which is close to the largest value to satisfy the above conditions. By this assumption, the volume fraction of the most dense condition with occupancy = 1 in the two-dimensional cell-based model is estimated as $\sim 41\%$ which is slightly large, but expected as the possible value in experimental situations (7).

If we regard the present model as the G-protein signal-transduction system, its time and spatial scales are estimated by considering the size of each cell to be of the same order as its molecular size, i.e., nm. The diffusion rate of particles was estimated as $\sim 10^{-1} - 10^{-2} \mu\text{m}^2/\text{s} = 10^{-1} - 10^{-2} \text{nm}^2/\mu\text{s}$ for the G-protein-coupled receptor without the cytoskeleton (34). Hence, the time interval between which a molecule moves a single molecule length is estimated as $\sim 10 - 100 \mu\text{s}$. We also assume that the 0.01–1 reactions occur for each molecule at each time step. This assumption gives the characteristic time for reactions as 0.1–10ms which is consis-

tent with the time scale of the conformational change of typical proteins.

Simulation method

To simulate the present cell-based model, we used the Monte-Carlo method. The temporal evolution of the system is progressed by the iteration of the following steps.

- (i) One of the cells is chosen randomly.
- (ii) If this cell contains a molecule R , R^* , S^* , or T , the corresponding reactions, 1, 2, 4, or 7, occur with the respective reaction rates. Here, reaction 7 indicates that T is removed from this cell.
- (iii) If this cell contains a molecule S or T , the corresponding two-body reactions, 3 or 6, occur with the rate given by the product of its [reaction rates] and [the number density of the corresponding catalyst on (six) neighboring cells]. Here, T^* is removed from this cell as soon as it appears.
- (iv) If this cell contains a molecule, but no reactions occur, this molecule moves to one of the neighboring (six) cells chosen randomly when the chosen cell is empty.
- (v) If this cell contains no molecules, the binding process of a target protein 5 occurs with the reaction rate P_{in} . This indicates that T is bound to this cell with the reaction rate P_{in} .

Here, the unit time step is given by the [Number of above iterations]/ N . We define the signal flow of the system, J , as the frequency of activation to unbind the target protein, where J at time t is given by [Number of activations of target proteins between t and $t + 1$].

RESULT AND DISCUSSION

Simulation result

In this section, the typical properties obtained through the simulation of the model, which the system includes no crowders, are considered. Firstly, we focus on the steady-state signal flow J , the frequency of activation of the target proteins, for several volume fractions of the signaling protein $[S_{tot}] = [S] + [S^*]$ and the binding probability of the target protein P_{in} . Here, $[X]$ means the volume fraction of the molecule X in the system. For simplicity, some parameters are fixed as follows: $k_S = 0.3$, $k_{S^*} = 0.3$, $k_T = 0.3$, and $[R_{tot}] = [R] + [R^*] = 0.25$. However, the following arguments are qualitatively independent of these details.

Fig. 3 shows J as a function of $[S_{tot}]$ and P_{in} for the set $(k_R, k_{R^*}, P_{out}) = (A) (1, 0, 0)$, $(B) (0.5, 0.5, 0)$, $(C) (0, 0, 0.3)$, and $(D) (0.5, 0.5, 0.3)$, Fig. 4 A gives the cross section of Fig 3 A which showing J as a function of P_{in} for several $[S_{tot}]$ ($0 \leq [S_{tot}] \leq 0.75$, because $[S_{tot}] + [R_{tot}] \leq 1$ and $[R_{tot}] = 0.25$). Together, these figures indicate that the signal flow J exhibits a maximum at $P_{in} = 1$ with the respective appropriate values of $[S_{tot}]$. The cases of $P_{in} = 1$ are such that a target protein binds to the membrane as soon as an empty space appears.

This further means that J exhibits a maximum in the case of a much higher total volume fraction of molecules, ρ , than that expected by mean-field analysis (see Appendix and Fig. 11 B). Here, at $[S_{tot}] = 0.25, 0.35$, and 0.65 , J increases linearly with ρ and exhibits a maximum at the maximum ρ for a given parameter set. It

should be noted that the diffusion of each molecule on the membrane is highly suppressed because most of the space is occupied by molecules in such cases of ρ such that J exhibits a maximum. Indeed, in the case of small $[S_{tot}]$, i.e., $[S_{tot}] = 0.025, 0.1$, J has a maximum peak at low ρ , such that each molecule can easily diffuse. However, influences of the molecular crowding, which generally suppress the reaction activity in three-dimensional bulk systems can lead to predominantly larger signal flows in the present reaction processes.

Spatial organization

As shown in above, the numerical results of the present model deviate considerably from those expected by mean-field analysis. This finding implies the existence of a spatially nonuniform distribution of molecular species, which can cause the higher signal flow enabled by a high volume fraction of molecules. Thus, to observe the characteristic spatial distributions of molecules, we measure the radial distribution function of each molecular species around each receptor.

The radial distribution functions of the receptor, signaling protein, and target protein around the receptor, $d_R(r)$, $d_S(r)$, and $d_T(r)$, are defined as

$$d_R(r) = \frac{\langle \rho_R(r) + \rho_{R^*}(r) \rangle}{[R_{tot}]}, \quad (8)$$

$$d_S(r) = \frac{\langle \rho_S(r) + \rho_{S^*}(r) \rangle}{[S_{tot}]}, \quad (9)$$

$$d_T(r) = \frac{\langle \rho_T(r) \rangle}{[T]}, \quad (10)$$

respectively. Here, $\rho_X(r)$ ($X = \{R, R^*, S, S^*, T\}$) indicates the volume fraction of molecules X in the region where the distance from the receptor is r , which is given as the minimum number of steps to move from the receptor to the molecule X . $\langle \rangle$ means the sample and the long-time averaged value. The molecule X is considered to accumulate when $d_X(r) > 1$, whereas X is considered sparse when $d_X(r) < 1$.

Firstly, we focus on the radial distribution functions when the system realizes the maximum signal flow. Fig. 5 shows the radial distributions of the receptor (plus), signaling protein (cross), and target protein (circle) as a function of distance from a receptor, r , with a large volume fraction of molecules such that J exhibits a maximum at $(k_R, k_{R^*}, P_{out}) = (1, 0, 0)$. This figure contains two regions divided by $r = r_c \approx 5$. For $r < r_c$, the distribution of target protein tends to be sparse, whereas receptors and signaling proteins tend to accumulate. On the other hand, for $r > r_c$, all molecules are uniformly distributed. Thus the molecules tend to distribute according to the following spatial structure: the signaling proteins surround the receptors, and the target proteins become distributed around the receptor–signaling protein cluster (Fig. 6).

If molecular distribution occurs according to the abovementioned structure, S around R^* and also T around S^* , tend to be activated rapidly. Thus, the reaction process of the present model progresses actively, even at a much higher volume fraction of molecules.

Moreover, the progress of such reaction processes is considered to contribute to the formation and sustainment of radial distributions in the following way. Once a signaling protein neighbors a receptor, the two tend to remain in the vicinity with

each other because the volume fraction of molecules is too high to diffuse them. Thus, as soon as the receptor is activated to be transformed into R , the signaling protein is activated to be transformed into S . Next, a T around this S is rapidly activated and unbound from the membrane. Soon, another T comes close to this S and is activated because the volume fraction of molecules is too high. These processes induce the flow of molecules from the distant location to the vicinity of the activated R , thereby sustaining the spatially ordered molecular distribution.

It should be noted that the formation of the present spatial structure is induced by the typical processes of signal transductions on biomembranes, e.g., binding, reactions, and unbinding of molecules, and also by the influences of molecular crowding. If the volume fraction of molecules is too small to allow smooth diffusion on the membrane, the abovementioned spatially ordered molecular distribution does not emerge.

Fig. 7 shows the radial distributions of each molecular species at $r = 1$ as a function of P_{in} . With decreases in P_{in} , regarded as decreases in the total volume fraction of molecules, the radial distributions at $r = 1$ become deviated from the case of a larger P_{in} . Although the target proteins tend to exist in the vicinity of the receptors, such a configuration does not contribute positively to signal flow because the receptors cannot directly activate the target protein. Moreover, such a distribution may often disturb the activation of signaling proteins by activated receptors. Thus, the reaction activity decreases in line with a decrease in P_{in} because of the breaking of the spatially ordered molecular distributions.

In other words, molecular flow is enhanced not diffusion, but by the spatial molecular ordering caused by influences of the molecular crowding. Thus, the reaction activity is increased.

Reaction system with crowding molecules

In the previous sections, we considered the ideal system, which is assumed to comprise only the components of the considered signal-transduction process. However, in general, several reaction processes are simultaneously progressed by several macromolecules on the cell membrane. The components progressing such a reaction process often behave as obstacles for the components progressing alternative reaction processes. Thus, to elucidate the influences of molecular crowding using a more realistic model of signaling processes on the membrane, we performed the simulation of the system containing the crowder molecule C , which moves randomly on the membrane without the reaction, binding, and unbinding. Here, C hinders the random movements of other reactive molecules because of its excluded volume. We consider the case of $[R_{tot}] = 0.25$ and $[C] = 0.3$, which is larger than or similar to the order of $[S_{tot}]$.

Fig. 8 shows J as a function of $[S_{tot}]$ and P_{in} for the set $(k_R, k_{R^*}, P_{out}) = (A) (1, 0, 0)$, $(B) (0.5, 0.5, 0)$, $(C) (1, 0, 0.3)$, and $(D) (0.5, 0.5, 0.3)$. Fig. 9, A and B and Fig. 10, A and B indicate the cross sections of Fig. 8, A and C for some $[S_{tot}]$ ($0 \leq [S_{tot}] \leq 0.4$, because $[S_{tot}] + [R_{tot}] + [C] \leq 1$). For the case of small P_{out} , as shown in Fig. 8, A and B and Fig. 9 A, J has a maximum peak at the certain $[S_{tot}]$ and P_{in} , which is much smaller than 1, in contrast to the system without C . However, P_{in} and the total volume fraction of molecules that exhibit a maximum J value are still much higher than those expected by mean-field approximations (Fig. 11 B). Moreover, in contrast to the results of mean-field approximations, J

continuously changes, and has a finite value is maintained at $P_{in} = 1$.

These data are explained as follows. As mentioned in the previous sections, the flow of molecules toward the receptor–signaling protein clusters (R - S clusters) emerges if the present reactions proceed in the presence of a high volume fraction of molecules. In such a case, not only the target proteins but also the crowders flow toward the R - S clusters. It should be noted that the target proteins tend to be unbound as soon as they come into contact with the R - S clusters, whereas the crowders tend to remain bound. With increase in the volume fraction, the crowders come close to the R - S clusters, thereby suppressing the activation of target proteins.

On the other hand, if the target proteins are frequently unbound from the membrane without activation, the emergence of empty spaces often enhances the exchange of positions between the target proteins and crowders. Thus, the surrounding probability of R - S clusters by crowders decreases, and target proteins can come close to the R - S clusters to be activated. The unbinding of target proteins without activation inevitably results in a certain loss of signal flow. However, based on an appropriate unbinding rate of target proteins P_{out} , we obtain the signal flow J , which exhibits the same qualitative properties as the J value obtained in the system without C (Fig. 3, C and D). It should be noted that it is natural for the model of reaction processes on biomembranes to assume that the unbinding rate of the target protein without activation has a finite value. Thus, molecular crowding generally tends to enhance the reaction activity in two-dimensional reaction systems such as signaling processes on biomembranes.

CONCLUSION

We investigated influences of the molecular crowding on the activity of reaction processes on two-dimensional surfaces, using the cell-based model of signal-transduction processes on the biomembranes. By simulation of the model based on the diffusion and reaction among receptors, signaling proteins, target proteins, and crowders on two-dimensional surface, we found that the signal flow exhibits a maximum value at a high volume fraction of molecules such that the diffusion of molecules is highly suppressed. We further demonstrated that such molecular crowding influences the hierarchical molecular distributions throughout the reaction process. The signaling proteins tend to surround the receptors, and the target proteins and crowders tend to become distributed around the receptor–signaling protein clusters. This distribution accelerates the receptor–signaling protein and the signaling protein–target protein reactions. The formation of such a spatial structure is induced by the restriction of diffusion by molecular crowding and also by the typical processes of signal transductions on biomembranes, e.g., binding, reactions, and unbinding of molecules. In this way, molecular crowding frequently enhances the reactions on two-dimensional surfaces, such as signaling processes on biomembranes, but suppresses reactions in three-dimensional bulk system.

To control the signal transduction activity on the membrane, we expect the formation of the presented hierarchical molecular distributions provide the dominant contribution as well as the receptor clustering (40). On the other hand, a large number of reaction processes other than the signaling cascade are known to progress on the interior and exterior surfaces of several biomembranes of internal organs such as the mitochondria, Golgi body, and nucleus. Based on our present

argument, we predict that the characteristics of such intracellular reaction dynamics in two-dimensional systems are effectively lower than those in three-dimensional space.

ACKNOWLEDGEMENT

The authors are grateful to Y. Togashi, K. Takahashi, K. Aoki, M. Nishikawa, M. Kikuchi for useful discussion and information. This work was supported by the Research Fellowship of the Japan Society for the Promotion of Science for Young Scientists to MF, by the Global COE Program G14 (Formation and Development of Mathematical Sciences Based on Modeling and Analysis) of MEXT of Japan to HN, and by the Grant-in-Aid for Scientific Research on Innovative Areas (Spying minority in biological phenomena (No.3306) (24115515)) of MEXT of Japan to AA.

APPENDIX: MEAN-FIELD APPROXIMATION

We analyzed the present model by the mean-field approximation, in a similar way to recent studies (14, 26). For simplicity, we showed only the results of the system without crowders because the results are qualitatively the same between systems with and without crowders. To compare the simulation results in the text, we used occupancy, and not volume fraction, as the index of molecular crowding. The relationship between occupancy and volume fraction is described in the text. The temporal evolution of the density of each molecular species, $[R]$, $[R^*]$, $[S^*]$, $[S]$ and $[T]$, is obtained by the modified mass action law involving the influences of the occupancy of molecules.

$$\frac{d[R]}{dt} = -k_R[R] + k_{R^*}[R^*] \quad (11)$$

$$\frac{d[R^*]}{dt} = k_R[R] - k_{R^*}[R^*] \quad (12)$$

$$\frac{d[S]}{dt} = -k_S f(\rho)[R^*][S] + k_{S^*}[S^*] \quad (13)$$

$$\frac{d[S^*]}{dt} = k_S f(\rho)[R^*][S] - k_{S^*}[S^*] \quad (14)$$

$$\frac{d[T]}{dt} = f(\rho)P_{in} - k_T f(\rho)[T][S^*] - P_{out}[T] \quad (15)$$

$$\rho = [S_{tot}] + [R_{tot}] + [T]. \quad (16)$$

Here, $f(\rho)$ denotes the occupancy, ρ , dependency of the collision rate of two reactive molecules. According to recent studies, $f(\rho)$ is chosen as a monotone decreasing function of ρ and implements $f(0) = 1$ and $f(1) = 0$, to represent the crowding effect (14, 26). Here, we employ $f(\rho) = 1 - \rho$ and consider the case of which the receptors are always active and the target proteins do not autonomously unbind from the membrane, i.e., $[R_{tot}] = [R^*]$ and $P_{out} = 0$. We can obtain the the same qualitative results independently of the details $f(\rho)$ and parameter sets.

From these equations, we estimate the steady-state signal flow, defined as the frequency of activation for unbinding of the target protein, $J = k_T f(\rho)[T][S^*]$. Fig. 11, A and B shows J as a function of the binding probability of the target protein,

P_{in} , and of the total volume fraction of molecules on the membrane ρ , respectively. In Fig. 11 A, the maximum peaks in J for several P_{in} are obtained in a very small region ($\sim 10^3$), and each J drops discontinuously to zero at each critical value. Moreover, as shown in Fig. 11 B, there exists a suitable intermediate value of total volume fraction of the molecules and a suitable mixing rate of each molecular species, to maximize J .

REFERENCES

1. Nishida, E., and Y. Gotoh. 1993. The MAP kinase cascade is essential for diverse signal transduction pathways. *Trends Biochem. Sci.* 18:128–131.
2. Saitoh, M., H. Nishitoh, M. Fujii, K. Takeda, K. Tobiume, Y. Sawada, M. Kawabata, K. Miyazono, and H. Ichijo. 1998. Mammalian thioredoxin is a direct inhibitor of apoptosis signal-regulating kinase (ASK) 1. *EMBO J.* 17:2596–2606.
3. Butler, A. A., S. Yakar, I. H. Gewolb, M. Karas, Y. Okubo, and D. LeRoith. 1998. Insulin-like growth factor-I receptor signal transduction: at the interface between physiology and cell biology. *Comp. Biochem. Physiol. B Biochem. Mol. Biol.* 121:19–26.
4. Chen, Z., T. B. Gibson, F. Robinson, L. Silvestro, G. Pearson, B.-e. Xu, A. Wright, C. Vanderbilt, and M. H. Cobb. 2001. MAP Kinases. *Chemical Reviews* 101:2449–2476.
5. Chang, L., and M. Karin. 2001. Mammalian MAP kinase signalling cascades. *Nature*. 410:37–40.
6. Qi, M., and E. A. Elion. 2005. MAP kinase pathways. *J. Cell Sci.* 118:3569–3572.
7. Fulton, A. B. 1982. How crowded is the cytoplasm? *Cell* 30:345–347.
8. Minton, A. P., G. C. Colclasure, and J. C. Parker. 1992. Model for the role of macromolecular crowding in regulation of cellular volume. *Proc. Natl. Acad. Sci. U.S.A.* 89:10504–10506.
9. Zimmerman, S. B., and A. P. Minton. 1993. Macromolecular crowding: biochemical, biophysical, and physiological consequences. *Annu. Rev. Biophys. Biomol. Struct.* 22:27–65.
10. Minton, A. P. 1998. Molecular crowding: analysis of effects of high concentrations of inert cosolutes on biochemical equilibria and rates in terms of volume exclusion. *Methods Enzymol.* 295:127–149.
11. Minton, A. P. 2001. The influence of macromolecular crowding and macromolecular confinement on biochemical reactions in physiological media. *J. Biol. Chem.* 276:10577–10580.
12. Ellis, R. J. 2001. Macromolecular crowding: an important but neglected aspect of the intracellular environment. *Curr. Opin. Struct. Biol.* 11:114–119.

13. Hall, D. 2003. Macromolecular crowding: qualitative and semiquantitative successes, quantitative challenges. *Biochim. Biophys. Acta, Proteins Proteomics* 1649:127–139.
14. Kim, J., and A. Yethiraj. 2009. Effect of macromolecular crowding on reaction rates: a computational and theoretical study. *Biophys. J.* 96:1333–1340.
15. Agrawal, M., S. B. Santra, R. Anand, and R. Swaminathan. 2009. Effect of macromolecular crowding on the rate of diffusion-limited enzymatic reaction. *Pramana* 71:359–368.
16. Jiao, M., H.-T. Li, J. Chen, A. P. Minton, and Y. Liang. 2010. Attractive protein-polymer interactions markedly alter the effect of macromolecular crowding on protein association equilibria. *Biophys. J.* 99:914–923.
17. Minton, A. P. 2010. Analysis of membrane binding equilibria of peripheral proteins: allowance for excluded area of bound protein. *Anal. Biochem.* 397:247–249.
18. Fritsch, C., and J. Langowski. 2011. Chromosome dynamics, molecular crowding, and diffusion in the interphase cell nucleus: a Monte Carlo lattice simulation study. *Chromosome Res.* 19:63–81.
19. Fernández, C., and A. P. Minton. 2011. Effect of nonadditive repulsive intermolecular interactions on the light scattering of concentrated protein-osmolyte mixtures. *J. Phys. Chem. B* 115:1289–1293.
20. Shtilerman, M. D., T. T. Ding, and P. T. Lansbury. 2002. Molecular crowding accelerates fibrillization of α -synuclein: could an Increase in the cytoplasmic protein concentration Induce Parkinson’s disease? *Biochemistry* 41:3855–3860.
21. Nagarajan, S., D. Amir, A. Grupi, D. P. Goldenberg, A. P. Minton, and E. Haas. 2011. Modulation of functionally significant conformational equilibria in adenylylate kinase by high concentrations of trimethylamine oxide attributed to volume exclusion. *Biophys. J.* 100:2991–2999.
22. Cheung, M., D. Klimov, and D. Thirumalai. 2005. Molecular crowding enhances native state stability and refolding rates of globular proteins. *Proc. Natl. Acad. Sci. U.S.A.* 102:4753–4758.
23. Kinjo, A., and S. Takada. 2002. Effects of macromolecular crowding on protein folding and aggregation studied by density functional theory: Dynamics. *Phys. Rev. E* 66:1–10.
24. Kilburn, D., J. H. Roh, L. Guo, R. M. Briber, and S. A. Woodson. 2010. Molecular crowding stabilizes folded RNA structure by the excluded volume effect. *J. Am. Chem. Soc.* 132:8690–8696.
25. Lin, J., A. Harding, E. Giurisato, and A. S. Shaw. 2009. KSR1 modulates the sensitivity of mitogen-activated protein kinase pathway activation in T cells without altering fundamental system outputs. *Mol. Cell. Biol.* 29:2082–2091.

26. Aoki, K., M. Yamada, K. Kunida, S. Yasuda, and M. Matsuda. 2011. Processive phosphorylation of ERK MAP kinase in mammalian cells. *Proc. Natl. Acad. Sci. U.S.A.* 108:12675–12680.
27. Lill, Y., K. L. Martinez, M. A. Lill, B. H. Meyer, H. Vogel, and B. Hecht. 2005. Kinetics of the initial steps of G protein-coupled receptor-mediated cellular signaling revealed by single-molecule imaging. *ChemPhysChem* 6:1633–1640.
28. Daumas, F., N. Destainville, C. Millot, A. Lopez, D. Dean, and L. Salomé. 2003. Confined diffusion without fences of a g-protein-coupled receptor as revealed by single particle tracking. *Biophys. J.* 84:356–366.
29. Matsuoka, S., T. Shibata, and M. Ueda. 2009. Statistical analysis of lateral diffusion and multistate kinetics in single-molecule imaging. *Biophys. J.* 97:1115–1124.
30. Miyanaga, Y., S. Matsuoka, T. Yanagida, and M. Ueda. 2007. Stochastic signal inputs for chemotactic response in *Dictyostelium* cells revealed by single molecule imaging techniques. *Bio Systems* 88:251–260.
31. Matsuoka, S., M. Iijima, T. M. Watanabe, H. Kuwayama, T. Yanagida, P. N. Devreotes, and M. Ueda. 2006. Single-molecule analysis of chemoattractant-stimulated membrane recruitment of a PH-domain-containing protein. *J. Cell Sci.* 119:1071–1079.
32. Saxton, M. J., and K. Jacobson. 1997. Single-particle tracking: applications to membrane dynamics. *Annu. Rev. Biophys. Biomol. Struct.* 26:373–399.
33. Mashanov, G. I., T. A. Nenasheva, M. Peckham, and J. E. Molloy. 2006. Cell biochemistry studied by single-molecule imaging. *Biochem. Soc. Trans.* 34:983–988.
34. Suzuki, K., K. Ritchie, E. Kajikawa, T. Fujiwara, and A. Kusumi. 2005. Rapid hop diffusion of a G-protein-coupled receptor in the plasma membrane as revealed by single-molecule techniques. *Biophys. J.* 88:3659–3680.
35. Kusumi, A., Y. Sako, and M. Yamamoto. 1993. Confined lateral diffusion of membrane receptors as studied by single particle tracking (nanovid microscopy). Effects of calcium-induced differentiation in cultured epithelial cells. *Biophys. J.* 65:2021–2040.
36. Fujiwara, T., K. Ritchie, H. Murakoshi, K. Jacobson, and A. Kusumi. 2002. Phospholipids undergo hop diffusion in compartmentalized cell membrane. *J. Cell Biol.* 157:1071–1081.
37. Nakada, C., K. Ritchie, Y. Oba, M. Nakamura, Y. Hotta, R. Iino, R. S. Kasai, K. Yamaguchi, T. Fujiwara, and A. Kusumi. 2003. Accumulation of anchored proteins forms membrane diffusion barriers during neuronal polarization. *Nat. Cell Biol.* 5:626–632.
38. Takahashi, K., S. Arjunan, and M. Tomita. 2005. Space in systems biology of signaling pathways-towards intracellular molecular crowding in silico. *FEBS Lett.* 579:1783–1788.

39. Bhide, S. Y., and S. Yashonath. 2000. Types of dependence of self-diffusivity on sorbate concentration in parameter space: a two-dimensional lattice gas study. *J. Phys. Chem. B* 104:2607–2612.
40. Bray, D., M. D. Levin, and C. J. Morton-Firth. 1998. Receptor clustering as a cellular mechanism to control sensitivity. *Nature* 393:85–88.

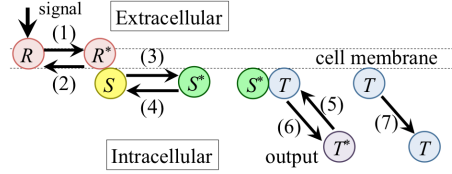


FIGURE 1 : Signaling pathway of this study. The signal is transferred via the activation of the receptor (Eq. 1), the activation of the signaling protein (Eq. 3), and the activation of the target protein with unbound (Eq. 6). The target protein in the cytoplasm stochastically becomes inactive and is rebound to the membrane (Eq. 5); the receptor and signaling protein also stochastically becomes inactive (Eqs. 2 and 4). The target protein on the membrane is stochastically unbound from the membrane (Eq. 7).

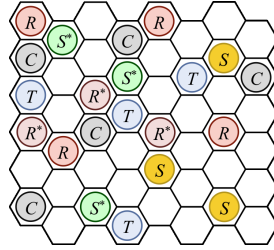


FIGURE 2 : Outline of the study model. The membrane is described as a hexagonal lattice surface. One cell can contain only one protein. R, R^*, S, S^*, T , and C indicate the inactive receptor, active receptor, inactive signaling protein, active signaling protein, target protein, and crowder, respectively.

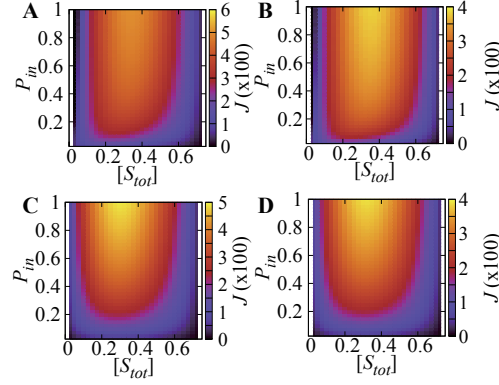


FIGURE 3 : Amplitude of signal flow J (color gradation) for $(k_R, k_{R^*}, P_{out}) = (A)$ $(1.0, 0, 0)$, (B) $(0.5, 0.5, 0)$, (C) $(1.0, 0, 0.3)$, and (D) $(0.5, 0.5, 0.3)$; and $[R_{tot}] = 0.25$ as a function of the volume fraction of the signaling protein $[S_{tot}]$ (horizontal axis) and the binding probability of the target protein P_{in} (vertical axis), respectively. The brighter color indicates the higher signal flow.

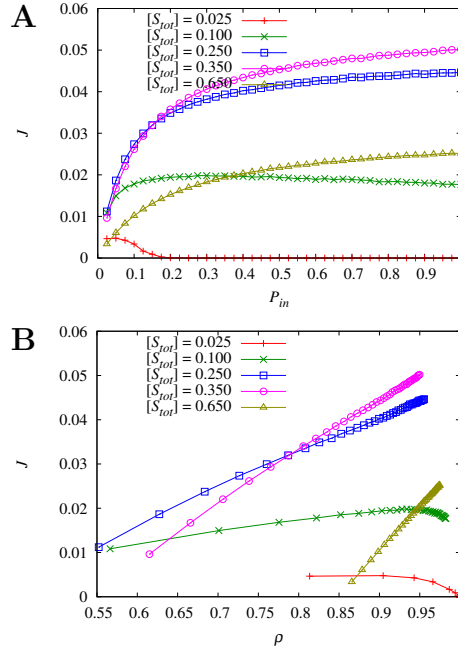


FIGURE 4 : Cross section of Fig. 3 A, showing J as a function of (A) P_{in} and (B) ρ for $[S_{tot}] = 0.025$ (red, +), 0.1 (green, \times), 0.25 (blue, \square), 0.35 (purple, \circ), and 0.65 (yellow, \triangle).

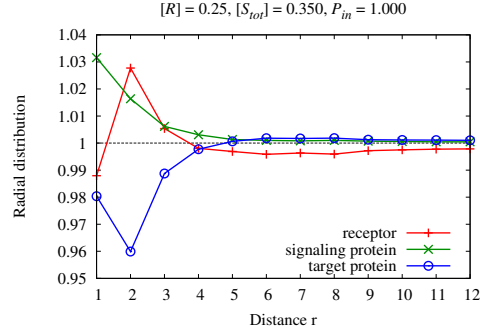


FIGURE 5 : Radial distributions around the receptor as functions of distance from receptor, r , for $[R_{tot}] = 0.25$, $[S_{tot}] = 0.35$, and $P_{in} = 1$, the combination realizing a maximum signal. The red (+), green (\times), and blue (\circ) lines indicate the radial distribution of the receptor ($d_R(r)$), signaling protein ($d_S(r)$), and target protein ($d_T(r)$) around the receptor, respectively.

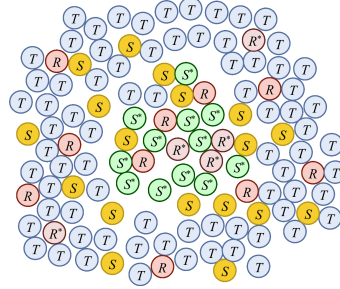


FIGURE 6 : Schematic diagram of spatial structure in the crowded condition with a high rate of signal flow.

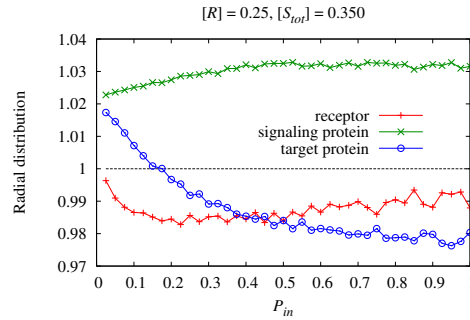


FIGURE 7 : Radial distributions around the receptor for $r = 1$, $d_R(1)$, $d_S(1)$, and $d_T(1)$, as functions of P_{in} when $[R] = 0.25$ and $[S_{tot}] = 0.35$. The red, green, and blue lines indicate $d_R(1)$, $d_S(1)$, and $d_T(1)$, respectively.

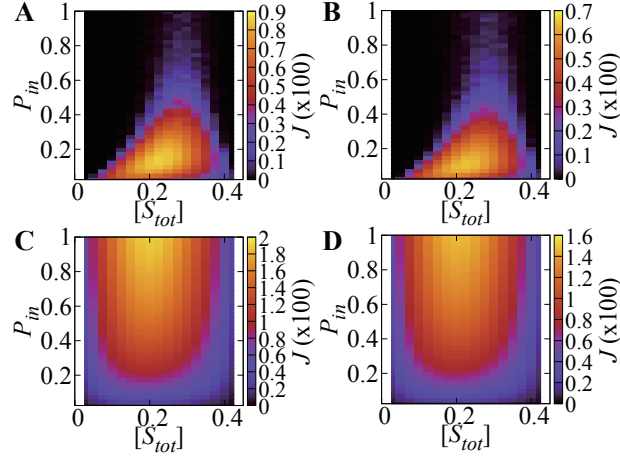


FIGURE 8 : Amplitude of signal flow J (color gradation) for $(k_R, k_{R^*}, P_{out}) = (A) (1.0, 0, 0)$, $(B) (0.5, 0.5, 0)$, $(C) (1.0, 0, 0.3)$, and $(D) (0.5, 0.5, 0.3)$; $[R_{tot}] = 0.25$, and $[C] = 0.3$ as a function of the volume fraction of the signaling protein $[S_{tot}]$ (horizontal axis) and the binding probability of the target protein P_{in} (vertical axis). The brighter color indicates the higher signal flow.

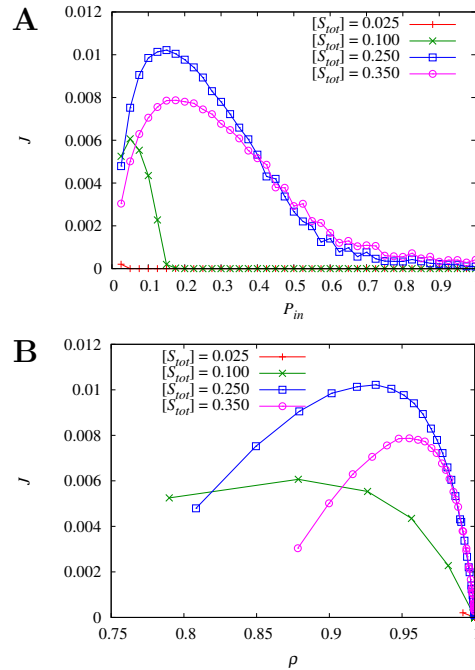


FIGURE 9 : Cross section of Fig. 8 A, showing J as a function of (A) P_{in} and (B) ρ for $[S_{tot}] = 0.025$ (red, +), 0.1 (green, \times), 0.25 (blue, \square), and 0.35 (purple, \bigcirc).

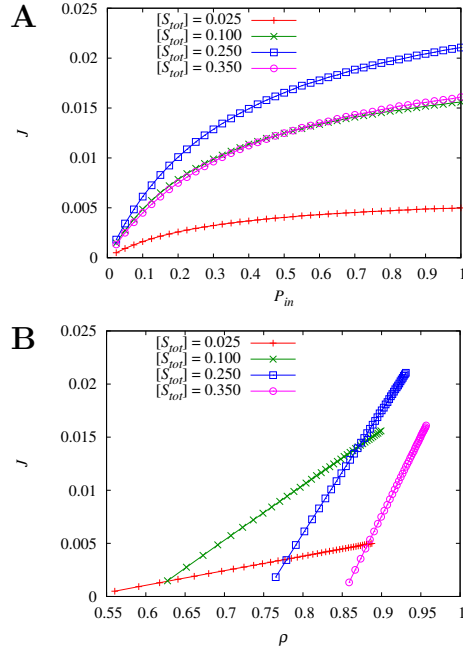


FIGURE 10 : Cross section of Fig. 8 C, showing J as a function of (A) P_{in} and (B) ρ for $[S_{tot}] = 0.025$ (red, +), 0.1 (green, x), 0.25 (blue, □), and 0.35 (purple, ○).

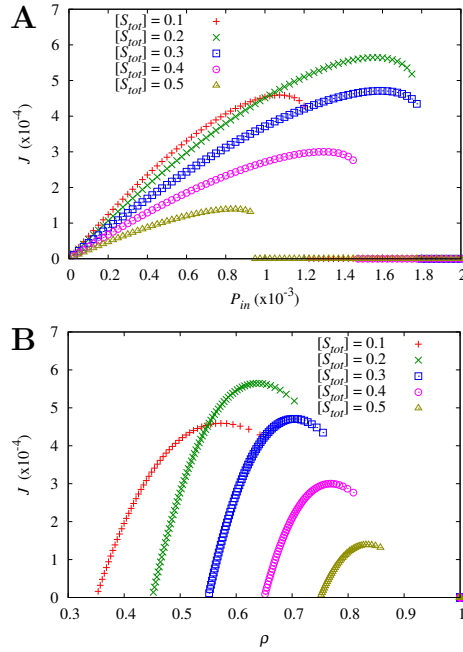


FIGURE 11 : Signal flow J obtained by mean-field approximation as a function of (A) $P_{in} (\times 10^{-3})$ and (B) ρ . $[S_{tot}] = 0.1$ (red, +), 0.2 (green, x), 0.3 (blue, □), 0.4 (purple, ○), and 0.5 (yellow, △).